Biochemical and Biophysical Research Communications 438 (2013) 666–672

Contents lists available at ScienceDirect

Biochemical and Biophysical Research Communications

journal homepage: www.elsevier.com/locate/ybbrc

Plasma membrane characterization, by scanning electron microscopy, of multipotent myoblasts-derived populations sorted using dielectrophoresis

Massimo Muratore [a,*], Steve Mitchell [b], Martin Waterfall [c]

[a] Institute of Integrated Micro and Nano System, School of Engineering, The University of Edinburgh, Edinburgh EH9 3JF, UK
[b] Institute of Molecular Plant Science, School of Biological Science, The University of Edinburgh, Edinburgh EH9 3JF, UK
[c] Institute of Immunology and Infection Research, School of Biological Science, The University of Edinburgh, Edinburgh EH9 3JT, UK

ARTICLE INFO

Article history:
Received 25 July 2013
Available online 7 August 2013

Keywords:
Dielectrophoresis
Plasma membrane capacitance
Multipotent cells

ABSTRACT

Multipotent progenitor cells have shown promise for use in biomedical applications and regenerative medicine. The implementation of such cells for clinical application requires a synchronized, phenotypically and/or genotypically, homogenous cell population. Here we have demonstrated the implementation of a biological tag-free dielectrophoretic device used for discrimination of multipotent myoblastic C2C12 model. The multipotent capabilities in differentiation, for these cells, diminishes with higher passage number, so for cultures above 70 passages only a small percentage of cells is able to differentiate into terminal myotubes. In this work we demonstrated that we could recover, above 96% purity, specific cell types from a mixed population of cells at high passage number without any biological tag using dielectrophoresis. The purity of the samples was confirmed by cytometric analysis using the cell specific marker embryonic myosin. To further investigate the dielectric properties of the cell plasma membrane we co-culture C2C12 with similar size, when in suspension, GFP-positive fibroblast as feeder layer. The level of separation between the cell types was above 98% purity which was confirmed by flow cytometry. These levels of separation are assumed to account for cell size and for the plasma membrane morphological differences between C2C12 and fibroblast unrelated to the stages of the cell cycle which was assessed by immunofluorescence staining. Plasma membrane conformational differences were further confirmed by scanning electron microscopy.

1. Introduction

Mesenchymal precursor's cells as C2C12 are model cells for regenerative studies due to their ability to differentiate into different cell types by means of chemical cues and/or factors, such insulin-like growth factors (IGFs), present in the culture medium [1–3]. C2C12 myoblasts represent a valuable system in studies investigating stem cell plasticity [4]. Although this ability has been shown related to cell age (passage number) [5–7]. These properties were exploited for studies in animal models in cardiomyogenesis grafts and cardiac cells transplantation [8,9] as well as other biomedical applications [4,10]. Altogether these results are very encouraging however the homogeneity and differentiation status of the cell population for regeneration remains problematic [11]. Dielectrophoresis (DEP) has been used for several biochemical and biomedical applications in order to fractionate and purify cells of interest from population of cells [10,12,13]. This technique has the advantage that it does not rely on any biological tag for cell separation and this absence of any biological manipulation is ideal for preserving the normal physiological conditions of the cells.

In this work we utilize DEP in a microfluidic device for high through output fractionation of cell population based on size and plasma membrane capacitance associated with the morphological organization of the plasma membrane.

DEP force on a spherical particle approximating a biological cell can be described by [14,15]:

$$F_{DEP} = 2\pi\varepsilon_m r^3 \mathrm{Re}(f_{CM}\omega)\nabla E_{rms}^2 \quad (1)$$

In Eq.(1) ε_m is the absolute permittivity of the medium, r is the radius of the cell, and f_{CM} is the real part of the Clausius–Mossotti (CM) factor which has limits between −0.5 and 1 and account for the frequency (ω) related complex permittivities ε_p^* and ε_m^* for the cell and medium respectively. E_{rms} is the strength of the electrical field. In Eq.(1) it is important to notice that DEP force is proportional to the volume of the particle and is dependent on the permittivity of surrounding medium, electrical properties of the particles and frequencies of the AC field [16].

When the CM is negative we have negative DEP (nDEP) which produce repulsion of the cells into area of low electrical field

* Corresponding author.
E-mail address: M.Muratore@ed.ac.uk (M. Muratore).

0006-291X/$ - see front matter © 2013 Elsevier Inc. All rights reserved.
http://dx.doi.org/10.1016/j.bbrc.2013.07.124

strength. In the opposite case, when the CM is positive, there is positive DEP (pDEP) and the cell is attracted to area of high region of field strength [17,18].

The transition between nDEP and pDEP is called cross-over frequency (f_{xo}) when the polarisability of the cell and medium are the same, this can is expressed by:

$$f_{xo} = \frac{\sqrt{2}\sigma_m}{2\pi r C_m} \quad (2)$$

Where the σ_m is the conductivity of the surrounding medium, r is the radius of the cell and C_m is the capacitance per unit area of the cell plasma membrane. For a completely smooth spherical cell the cell membrane capacitance can be expressed as [19,20]:

$$C_m = \frac{\varepsilon_m \varepsilon_o}{d} \quad (3)$$

with d and ε as the thickness and permittivity of the membrane respectively. The total membrane capacitance (C_t) is defined as [19]:

$$C_t = 4\pi r^2 C_m \quad (4)$$

For erythrocytes the values of the plasma membrane capacitance has been extrapolated in several studies as 6–8 mF/m^2 [21–23]. The values for C_m have been evaluated in cells presenting projection and other morphological bound extensions on the plasma membrane resulting in higher values [12,19,24,25]. This demonstrates correlation between the C_m and the overall roughness of the cell plasma membrane and the presence of projection/microvilli [19]. The presence of microvilli is common; with variations in length and number due to cell's environmental conditions and/or cellular adaptations associated with differentiation/function [19,26,27]. Asami used finite elements methods for numerical simulation of changes, during osmotic perturbation, of the dielectric properties of bound microvilli in the cell plasma membrane [19]. However, it has also been shown that the presence of proteins of different sizes and that perturbations created by proteins-lipids bilayer interactions may play an important role in membrane capacitance [10,28,29].

In order to sort high purified cell types from a mix population we used a microfluidic device as illustrated in Supplementary Fig. 1 (S1). We used frequencies different values to separate cell types based on the cross-over frequencies determined in previous work [10].

Purity of the sorted samples was assessed using flow cytometry analysis to detect the presence of GFP (fibroblasts) or embryonic myosin which is specific for myotubes and is not expressed by C2C12 undifferentiated myoblasts [30–34].

Here the focus was to identify the characteristics of the cells which may be responsible for high level of purification achieved by DEP-sorting. We therefore analyzed the size cell in suspension as they would be for sorting and differences in the plasma membrane conformations between C2C12 myoblasts/myotubes and GFP-fibroblasts. Finally we use immunostaining to detect any differences in cell cycle stages between the cell types for possible correlations with sorting efficiency.

2. Materials and methods

All chemicals and reagents were purchased from Sigma (Poole, UK) unless otherwise stated.

2.1. Cell culture

2.1.1. C2C12 mouse myoblast cell line

C2C12 cells at high passage number (>70) were seeded at a starting density of 3000 cells/cm^2 and grown in high glucose DMEM growth medium (GM) supplemented with 10% FBS (HyClone), 2 mM of L-glutamine, 100 units/ml of penicillin and 100 μg/ml streptomycin sulphate (Invitrogen). Cells were passaged while at low confluence and induced to myogenic differentiation when above 90% confluence. The differentiation medium (DM), changed every other day, comprised high glucose DMEM, 0.1% FBS (Hyclone), 100 units/ml of penicillin and 100 μg/ml streptomycin sulphate (Invitrogen), 5 μg/ml transferrin and 10 μg/ml insulin. All cultures were maintained at 37 °C with 5% CO_2.

2.1.2. Co-culture of C2C12 and MRC-5 (GFP-fibroblast cell line)

Fibroblasts cells are cultured in the presence of puromycin to maintain selection for GFP selection. Therefore C2C12 were initially cultured in the presence of 2 μg/ml of puromycin in the medium to assess possible toxicity of the compound to the myoblasts. No alterations in phenotype, morphology or anomalies in expression of embryonic myosin were seen in the C2C12 cultures exposed to this concentration of puromycin. We therefore proceeded to co-culture C2C12 and GFP-fibroblasts (the cells were a donation from Dr. Joe Burrage) in GM supplemented with 2 μg/ml of puromycin for a week before analysis. GFP expression in fibroblasts allow them to be distinguished from C2C12 myoblasts by flow cytometry.

2.2. Flow cytometry analysis

Samples were analyzed as described in previous work [10] using the expression of GFP by fibroblasts and embryonic myosin for myotube detection. For cell cycle analysis the cells sorted by DEP were washed in Flow permeabilisation buffer (F-PBS) composed of phosphate buffer solution (PBS Mg^{++}–, Ca^{++}–free) supplemented with 0.1% BSA V and 0.1% NaN_3 azide. Cells were permeabilised by addition of an equal volume of cold 70% ethanol solution followed vortexing. After overnight incubation at −20 °C, cells were pelleted and then washed twice by centrifugation at 2000 rpm for 5 min, before the addition of RNase (100 μg/ml). Cells were incubated for one hour at room temperature and finally Propidium Iodine (PI) was added at concentration of 50 μl/ml.

Samples were analyzed using a LSRII flow cytometer (Beckton Dickinson Immunocytometry Systems, UK) running BD FACSDiva v6 Software. An electronic acquisition gate was applied to the forward/side scatter (FSC/SSC) plot to exclude debris from intact material and typically more than 50,000 events were acquired in this gate. Analysis was performed using FlowJo software (Tree Star, USA). Debris was excluded through FSC/SSC profile gating before applying electronic gates to assess green fluorescence. Sort purity was calculated by application of gates generated using profiles from each cell type alone as controls.

2.3. Scanning electron microscopy (SEM) preparations

Samples of individual cell types were fixed in a solution of 3% glutaraldehyde in 0.1 M sodium cacodylate buffer (pH 7.3) for 2 h before washing in three changes of 0.1 M sodium cacodylate buffer, each for 10 min. Samples were then postfixed in 1% osmium tetroxide in 0.1 M sodium cacodylate buffer for 45 min. A further 3 × 10 min washes were performed in 0.1 M sodium cacodylate buffer. Dehydration in graded concentrations of acetone (50%, 70%, 90%, and 3 × 100%) for 10 min each was followed by critical point drying using liquid carbon dioxide. After mounting on aluminium stubs with carbon tabs attached, the specimens were sputter coated with 20 nm gold palladium and viewed using a Hitachi S-4700 scanning electron microscope. Images were color-enhanced to highlight differences in the microvilli structure between cell types.

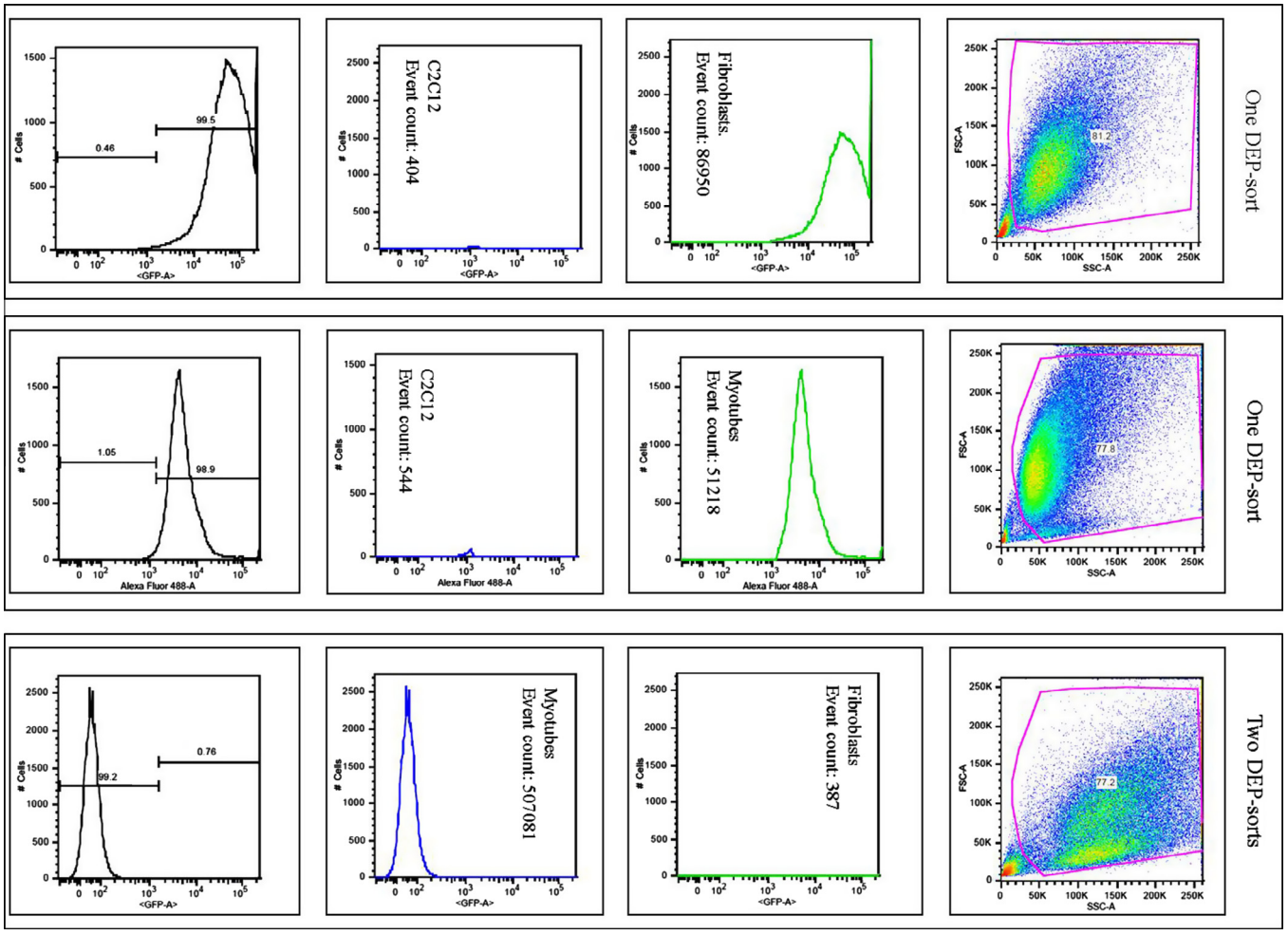

Fig. 1. Flow cytometry profiles of DEP-sorted C2C12, Fibroblasts GFP+ and myotubes. Percentage purities of separated populations are indicated in the first graphs on the left hand side. The top row shows an example of the level of separation between C2C12 and fibroblasts co-cultured after DEP sorting; for all the experiments the mean level of purity for these two cell types was ~98%. Middle row shows an example of the level of separation between C2C12 and Myotubes from a mixed and induced population after DEP sorting; for all the experiments the mean level of purity for these two cell types was ~96%. Bottom row shows the level of separation between myotubes and fibroblast after an initial sorting of both cell types from C2C12. The cells were sorted twice from several mixed populations.

2.4. Immunostaining

Cells were fixed in 3.7% formaldehyde. Then washed three times for five minutes each in TBS washing solution composed of Tris 50 mM, NaCl 150 mM and 0.1% Tween 20 at pH 7.4. Ki-67 (BDbiosciences) was added in blocking solution composed of TBS, 0.1% Tween-20 and 0.9% Fish gelatine. After incubation at room temperature (RT) for an hour cells were washed in TBS solution three times for five minutes each. Secondary antibodies diluted in blocking buffer were added for one hour at RT. Secondary antibodies used were: for C2C12 and myotubes Alexa Fluor 488 was used and Alexa Fluor 578 for GFP + Fibroblasts.

Cells were washed twice for five minutes each in washing solution before addition of DAPI nuclear dye for ten minutes at 37 °C. Finally cells were washed in PBS twice for five minutes each and the slides were mounted using Vectashield mounting medium. Cover slips were sealed and imaged with fluorescent microscope.

2.5. DEP Device

Details of the DEP device are shown in Supplementary Fig. S1a this is a modified version in geometry of similar devices used in other studies [15,35–37]. The electrodes generate the electric field necessary for DEP separation. The geometry of the electrodes is symmetrical and is composed of three sets of five electrodes with gaps between sets of 100, 75 and 50 μm to funnel the cells of interest in the central outlet for collection as illustrated in Supplementary Fig. S2a. The electrodes were fabricated by evaporation of 20 nm of Titanium on glass substrate follow by 200 nm of platinum using lift-off process. The walls of the micro-channel were realized by photolithographic process using SU-8. The angle of the electrodes was at 18° degrees in the direction of the fluid flow. The chip was mounted on a custom made holder containing ports for the inlets and outlets and electrical connections. Two syringe pumps (Harvard apparatus) were used to introduce the cells suspended in DEP-medium into the two outer inlets and DEP medium only into the central inlet. Simulation of the cell trajectory was produced using Comsol Multiphysics (version 4.3b) as shown in Supplementary Fig. S2b.

The population of mixed cells was re-suspended in DEP medium with a conductivity of ~120 mS/m and osmolarity ~330 mOsm/kg.

3. Results

3.1. Flow cytometry analysis of DEP-sorted populations

After the cells were harvested they were re-suspended in DEP-medium and loaded into the syringe pump for DEP-sorting. Purity

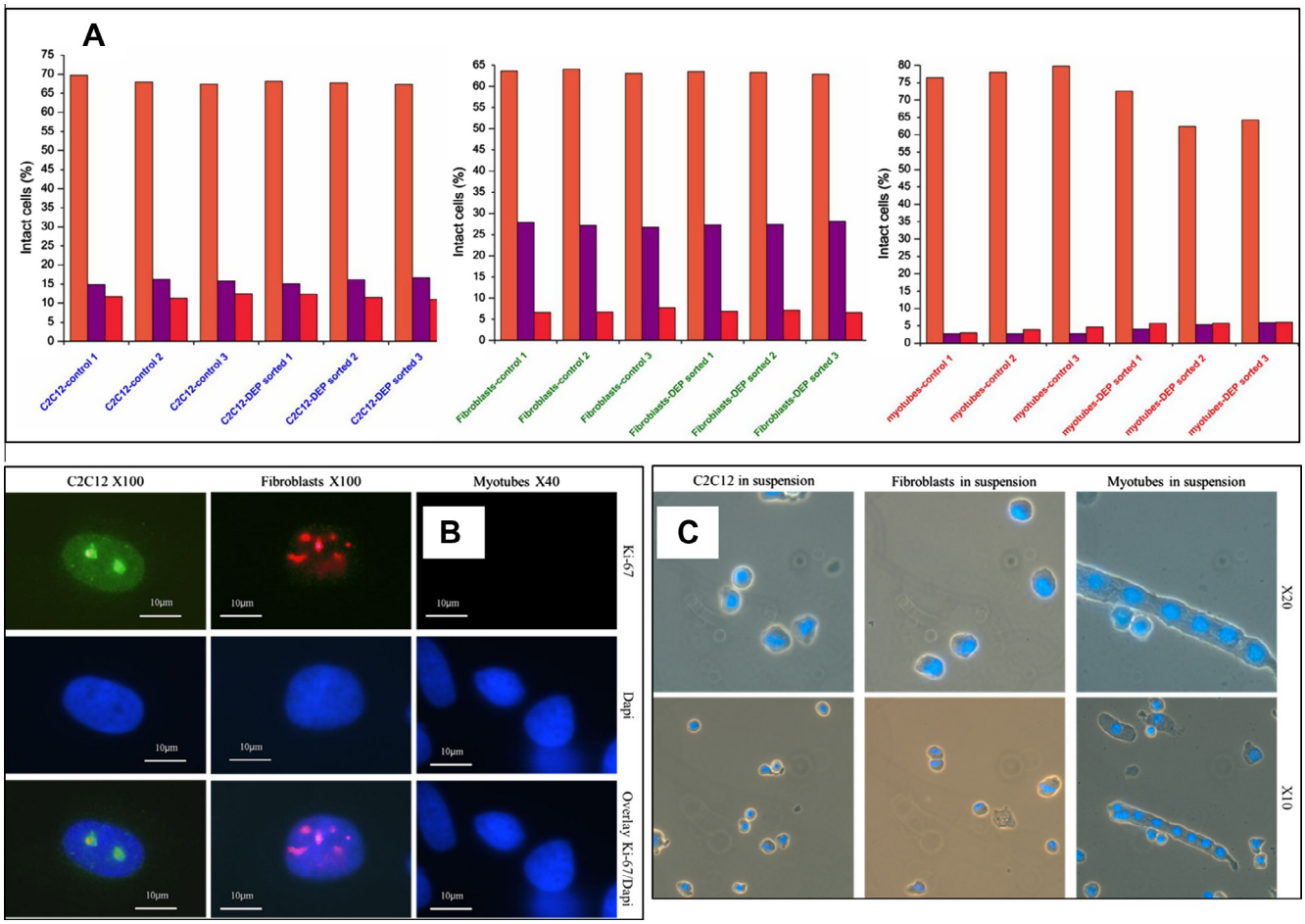

Fig. 2. (A) Shows the flow analysis of the cell cycle of the three cell types before and after DEP sorting. (B) Immunostaining for Ki-67 (described in Material and Methods) for cell cycling, DAPI nuclear stain was used as reference for better visualization. Both C2C12 and fibroblast are positive for Ki-67 (cell cycle active 1a and 2a) where myotubes are negative (third column 2b). Third row is an overlay of Ki-67 and DAPI staining. (C) An example of cell size when in suspension by contrast microscopy images using Hoechst nuclear dye for localization of the nucleus. Both C2C12 and fibroblasts showed similar size in suspension (first two columns of Fig. 2C).

and identity of the recovered sub-populations was assessed by flow cytometry, based on GFP-positivity (fibroblasts), the presence of embryonic myosin (C2C12 differentiated myotubes: secondary Alexa-Fluor 488) or non-fluorescence (C2C12 undifferentiated myoblasts). The experiments were in triplicate for 13 separate samples. Representative results are shown in Fig. 1. Cytometry plots in row 1 illustrate separation at 98% purity, following one round of DEP-sorting, of co-cultured GFP-positive fibroblasts from undifferentiated C2C12 myoblasts. At high passage number (>70) only a small percentage of C2C12 myoblasts will differentiate to myotubes. Following induction of differentiation we were able to DEP-sort induced myotubes from C2C12 at purity ~96% as illustrated by flow cytometry results in the second row in Fig. 1. Having successfully DEP-sorted C2C12 myoblasts from both fibroblasts and myotubes to high purity, we applied DEP-sorting to separation of fibroblasts and myotubes.

Co-cultures of fibroblasts andC2C12 myoblasts or cultures of differentiated C2C12 cells (containing myoblasts and myotubes) were each subjected to a first round of DEP-sorting to collect respectively from each. After the first collection fibroblasts and myotubes were mixed and a second round of DEP sorting was used to collect separate cell population of myotubes (from several cultures) or fibroblasts. Purity of recovered cells was assessed using GFP to identify fibroblasts as illustrated by the flow cytometry results in third row of Fig. 1.

3.2. Cell cycle: flow cytometry and immunofluorescence analysis

The second part of the study examined the possibility that separation of the cell types used in the study correlate with the cell cycle, since DEP has been used to sort cells based on their cell cycle stage [38]. The flow cytometry results are illustrated in Fig. 2A by histograms showing the intact cells collected in G0/G1, S and G2/M phase. All cultures analyzed showed a very similar profile before and after DEP sorting for C2C12 and fibroblasts as shown in the first two histograms from the left in Fig 2A. C2C12-derived myotubes, as expected, showed a synchronicity in G1 phase, due to the fact that these cells are differentiated and so are withdrawn from the cell cycle [7,39,40] as shown in histograms on the right hand side of Fig. 2A. To further validate these results we stained the DEP-sorted cells with Ki-67 to determine cell cycling activity, as illustrated in Fig. 2B. Both C2C12 and fibroblasts were positive for Ki-67 (Fig. 2B first two columns on the left) with myotubes negative as indicated in Fig. 2B (picture 3a). To determine size differences between the three cell types we used Hoechst nuclear dye with contrast microscopy as shown in Fig. 2C. The size validation between C2C12 and fibroblasts was important to determine if the DEP capability for sorting cells was solely dependent on cell size or if plasma membrane conformation was also responsible. It is evident in Fig. 2C that the C2C12-derive myotubes are much larger and are multinucleated in comparison to both C2C12 and fibro-

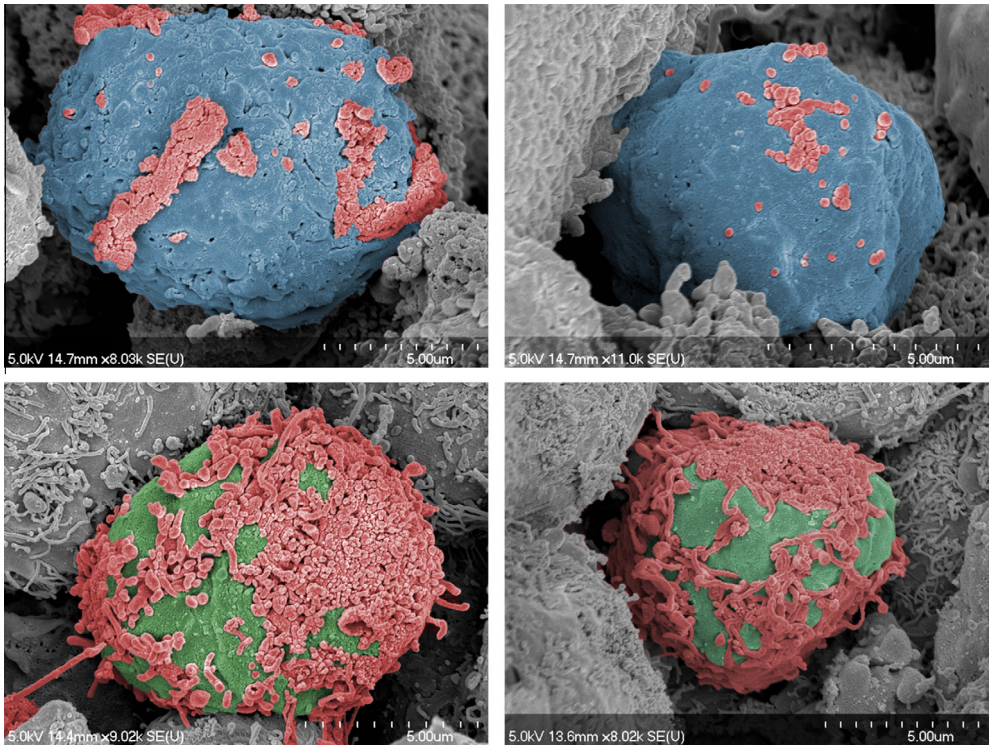

Fig. 3. SEM images of C2C12 (blue–red) and fibroblasts (green–red). The colors have been enhanced for better visualization. The microvilli are colored in red and the underling surface is colored in blue for C2C12 and green for fibroblast. The quantities and conformation of the microvilli are more pronounced on fibroblast (bottom two pictures). (For interpretation of the references to color in this figure legend, the reader is referred to the web version of this article.)

blasts. Also, in Fig. 2C is a representative sample showing size differences between C2C12 and fibroblasts. Images were collected of these two cell types in suspension and Image J software was used to determine size differences.

The averages for C2C12 myoblast was 18.6 μm ± 5.8 SD in diameter (1500 cells counted) and fibroblasts 18.9 μm ± 7.4 SD in diameter (1500 cells counted).

3.3. SEM analysis

To verify structural differences of microvilli between cells of similar size (C2C12 myoblasts and fibroblasts) SEM microscopy was used, results are shown in Figs. 3 and 4. In Fig. 3 image of cells in suspension as they would be for sorting are shown. As can be seen C2C12 myoblasts (blue–red colors) have an apparently less elaborate microvilli structure compared with fibroblast (green–red colors). The images have been color enhanced to highlight the differences in the quantity and conformation of microvilli in the two cell types. However although it is apparent that the difference between the two cell types is pronounced, exact quantification remain difficult.

To further compare the two cell types SEM images of attached cells, as cells would be during culture were analyzed as shown in Fig. 4. Here in low magnification images (top row Fig. 4) the microvilli structure was difficult to assess although a clear difference in phenotypical shape is present in these two cell types when attached. At higher magnification, in Fig. 4 bottom row, it is possible to see differences in plasma membrane structure between C2C12 (left) and fibroblasts (right), again the C2C12 myoblasts are apparently smoother than fibroblasts.

4. Discussions

DEP was very efficient in sorting all mixed populations of cells used in this study.

Differences in cross-over frequencies were the discriminatory tool used to achieve high levels of separation between the three cell types used (Fig. 1), as demonstrated in our previous study [10]. Analysis of the cell size and "smoothness" by light microscopy and SEM respectively showed that there were differences between the cell types used. C2C12 myoblasts and induced myotubes mainly differed in size shown in Fig. 2C. Whereas fibroblasts and C2C12 were found to have very different plasma microvilli arrangements, with fibroblasts having apparently many more villi. This difference in the cell surface could be responsible for changes in membrane capacitance and cross-over frequency.

We did not find any statistical difference between the stage of the cell cycle before and after DEP sorting; we can conclude that if there is a change in size during stages of cell cycle it is not sufficient to account for the separation shown in Fig. 1. Though DEP-sorting based on cell cycle stage has been reported it is possible that since here mammalian cells were used the correlation between cell cycle stage and size may be not the applicable, as for example is the case in yeast cells.

The SEM analysis of cell membrane microvilli landscape and conformation revealed a visible difference between C2C12 myoblasts both in suspension and attached as illustrated in Fig 3 and 4. Thus it is possible that differences in morphology of the cell surface were probably responsible for differences in plasma membrane capacitance and cross-over frequency between these two cells type.

Overall we can conclude that DEP sorting between these three types of cells is probably due to size and plasma membrane microvilli quantity and conformation.

Acknowledgments

We want to thank Prof Ron Pethig, Dr. Vlastimil Srsen, Dr. Kay K. Samuel and Dr Andreas Tsiamis for the helpful discussions.

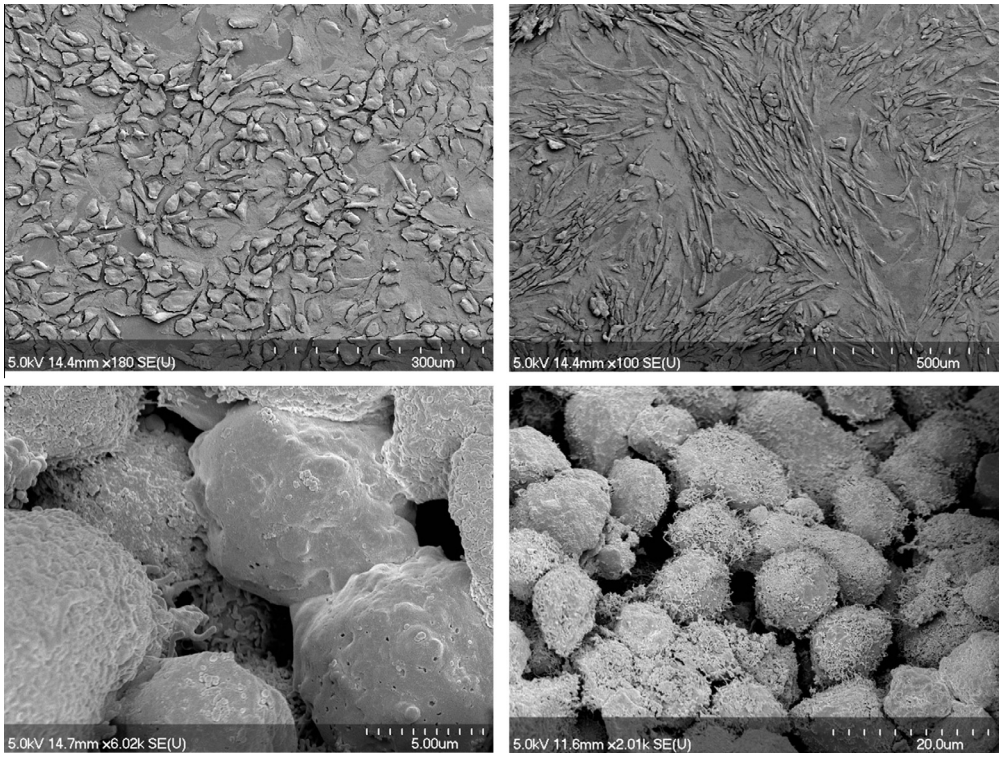

Fig. 4. C2C12 myoblasts (left column) and fibroblasts (right column) overall view of attached cells by SEM microscopy. The fibroblasts on the right of the above figure shows more microvilli structure compared with a less villous/more smooth morphology of C2C12 overall.

Appendix A. Supplementary data

Supplementary data associated with this article can be found, in the online version, at http://dx.doi.org/10.1016/j.bbrc.2013.07.124.

References

[1] S. Chen, S. Takanashi, Q. Zhang, W. Xiong, S. Zhu, E.C. Peters, S. Ding, P.G. Schultz, Reversine increases the plasticity of lineage-committed mammalian cells, Proceedings of the National Academy of Sciences 104 (2007) 10482–10487.

[2] Y. Xu, Y. Shi, S. Ding, A chemical approach to stem-cell biology and regenerative medicine, Nature 453 (2008) 338–344.

[3] Y. Yoshiko, K. Hirao, N. Maeda, Differentiation in C2C12 myoblasts depends on the expression of endogenous IGFs and not serum depletion, American Journal of Physiology - Cell Physiology 283 (2002) C1278–C1286.

[4] Y. Watanabe, S. Kameoka, V. Gopalakrishnan, K.D. Aldape, Z.Z. Pan, F.F. Lang, S. Majumder, Conversion of myoblasts to physiologically active neuronal phenotype, Genes & Development 18 (2004) 889–900.

[5] E. Schultz, B.H. Lipton, Skeletal muscle satellite cells: Changes in proliferation potential as a function of age, Mechanisms of Ageing and Development 20 (1982) 377–383.

[6] M.C. Gibson, E. Schultz, Age-related differences in absolute numbers of skeletal muscle satellite cells, Muscle & Nerve 6 (1983) 574–580.

[7] A.P. Sharples, N. Al-Shanti, M.P. Lewis, C.E. Stewart, Reduction of myoblast differentiation following multiple population doublings in mouse C2C12 cells: A model to investigate ageing?, Journal of Cellular Biochemistry 112 (2011) 3773–3785

[8] G.Y. Koh, M.G. Klug, M.H. Soonpaa, L.J. Field, Differentiation and long-term survival of C2C12 myoblast grafts in heart, The Journal of Clinical Investigation 92 (1993) 1548–1554.

[9] R.B. Thompson, S.M. Emani, B.H. Davis, E.J. van den Bos, Y. Morimoto, D. Craig, D. Glower, D.A. Taylor, Comparison of Intracardiac Cell Transplantation: Autologous Skeletal Myoblasts Versus Bone Marrow Cells, Circulation 108 (2003) 264–271.

[10] M. Muratore, V. Srsen, M. Waterfall, A. Downes, R. Pethig, Biomarker-free dielectrophoretic sorting of differentiating myoblast multipotent progenitor cells and their membrane analysis by Raman spectroscopy, Biomicrofluidics 6 (2012) 034113.

[11] X.L. Aranguren, J.D. McCue, B. Hendrickx, X.-H. Zhu, F. Du, E. Chen, B. Pelacho, Pe, xF, I. uelas, G. Abizanda, M. Uriz, S.A. Frommer, J.J. Ross, B.A. Schroeder, M.S. Seaborn, J.R. Adney, J. Hagenbrock, N.H. Harris, Y. Zhang, X. Zhang, M.H. Nelson-Holte, Y. Jiang, A.D. Billiau, W. Chen, Pr, F. sper, C.M. Verfaillie, A. Luttun, Multipotent adult progenitor cells sustain function of ischemic limbs in mice, The Journal of Clinical Investigation 118 (2008) 505–514.

[12] X.-B. Wang, Y. Huang, P.R.C. Gascoyne, F.F. Becker, R. Hölzel, R. Pethig, Changes in Friend murine erythroleukaemia cell membranes during induced differentiation determined by electrorotation, Biochimica et Biophysica Acta (BBA) - Biomembranes 1193 (1994) 330–344.

[13] Z.R. Gagnon, Cellular dielectrophoresis: Applications to the characterization, manipulation, separation and patterning of cells, Electrophoresis 32 (2011) 2466–2487.

[14] P.R.C. Gascoyne, J. Vykoukal, Particle separation by dielectrophoresis, Electrophoresis 23 (2002) 1973–1983.

[15] X. Hu, P.H. Bessette, J. Qian, C.D. Meinhart, P.S. Daugherty, H.T. Soh, Marker-specific sorting of rare cells using dielectrophoresis, Proceedings of the National Academy of Sciences of the United States of America 102 (2005) 15757–15761.

[16] J. Voldman, Electrical Forces For Microscale Cell Manipulation, Annual Review of Biomedical Engineering 8 (2006) 425–454.

[17] T.B. Jones, Electromechanics of Particles, Cambridge University Press, 1995.

[18] H. Pohl, Dielectrophoresis: The behaviour of neutral matter in nonuniform electric fields, Cambridge University Press, 1978.

[19] K. Asami, Dielectric properties of microvillous cells simulated by the three-dimensional finite-element method, Bioelectrochemistry 81 (2011) 28–33.

[20] A.L. Garner, G. Chen, N. Chen, V. Sridhara, J.F. Kolb, R.J. Swanson, S.J. Beebe, R.P. Joshi, K.H. Schoenbach, Ultrashort electric pulse induced changes in cellular dielectric properties, Biochemical and Biophysical Research Communications 362 (2007) 139–144.

[21] S. Takashima, K. Asami, Y. Takahashi, Frequency domain studies of impedance characteristics of biological cells using micropipet technique. I. Erythrocyte, Biophysical Journal 54 (1988) 995–1000.

[22] K. Asami, Y. Takahashi, S. Takashima, Dielectric properties of mouse lymphocytes and erythrocytes, Biochimica et Biophysica Acta (BBA) - Molecular, Cell Research 1010 (1989) 49–55.

[23] R. Lisin, B. Zion Ginzburg, M. Schlesinger, Y. Feldman, Time domain dielectric spectroscopy study of human cells. I. Erythrocytes and ghosts, Biochimica et Biophysica Acta (BBA) -, Biomembranes 1280 (1996) 34–40.

[24] A. Irimajiri, K. Asami, T. Ichinowatari, Y. Kinoshita, Passive electrical properties of the membrane and cytoplasm of cultured rat basophil leukemia cells. II. Effects of osmotic perturbation, Biochimica et Biophysica Acta (BBA) -, Biomembranes 896 (1987) 214–223.

[25] F.H. Labeed, H.M. Coley, M.P Hughes, Differences in the biophysical properties of membrane and cytoplasmof apoptptic cells revealed using dielectrophoresis, Biochimica et Biophysica Acta (BBA) - General Subjects 896 (1987) 214–223.

[26] B. Alberts, A. Johnson, J. Lewis, M. Raff, K. Roberts, P, Walter, Molecular biology of the cell, Garland, 2002.

[27] K. Ratanachoo, P.R.C. Gascoyne, M. Ruchirawat, Detection of cellular responses to toxicants by dielectrophoresis, Biochimica et Biophysica Acta (BBA), Biomembranes 1564 (2002) 449–458.
[28] D. Zimmermann, A. Zhou, M. Kiesel, K. Feldbauer, U. Terpitz, W. Haase, T. Schneider-Hohendorf, E. Bamberg, V.L. Sukhorukov, Effects on capacitance by overexpression of membrane proteins, Biochemical and Biophysical Research Communications 369 (2008) 1022–1026.
[29] M. Venturoli, B. Smit, M.M. Sperotto, Simulation Studies of Protein-Induced Bilayer Deformations, and Lipid-Induced Protein Tilting, on a Mesoscopic Model for Lipid Bilayers with Embedded Proteins, Biophysical Journal 88 (2005) 1778–1798.
[30] F. Edom-Vovard, V. Mouly, J.P. Barbet, G.S. Butler-Browne, The four populations of myoblasts involved in human limb muscle formation are present from the onset of primary myotube formation, Journal of Cell Science 112 (1999) 191–199.
[31] C. Webster, L. Silberstein, A.P. Hays, H.M. Blau, Fast muscle fibers are preferentially affected in Duchenne muscular dystrophy, Cell 52 (1988) 503–513.
[32] S. Schiaffino, L. Gorza, S. Sartore, L. Saggin, M. Carli, Embryonic myosin heavy chain as a differentiation marker of developing human skeletal muscle and rhabdomyosarcoma: A monoclonal antibody study, Experimental Cell Research 163 (1986) 211–220.
[33] S.M. Hughes, H.M. Blau, Muscle fiber pattern is independent of cell lineage in postnatal rodent development, Cell 68 (1992) 659–671.
[34] C.P. Emerson Jr, S.K. Beckner, Activation of myosin synthesis in fusing and mononucleated myoblasts, Journal of Molecular Biology 93 (1975) 431–447.
[35] S. Fiedler, S.G. Shirley, T. Schnelle, G. Fuhr, Dielectrophoretic Sorting of Particles and Cells in a Microsystem, Analytical Chemistry 70 (1998) 1909–1915.
[36] T. Müller, G. Gradl, S. Howitz, S. Shirley, T. Schnelle, G. Fuhr, A 3-D microelectrode system for handling and caging single cells and particles, Biosensors and Bioelectronics 14 (1999) 247–256.
[37] S. Burgarella, S. Merlo, B. Dell'Anna, G. Zarola, M. Bianchessi, A modular microfluidic platform for cells handling by dielectrophoresis, Microelectronic Engineering 87 (2010) 2124–2133.
[38] U. Kim, C.-W. Shu, K.Y. Dane, P.S. Daugherty, J.Y.J. Wang, H.T. Soh, Selection of mammalian cells based on their cell-cycle phase using dielectrophoresis, Proceedings of the National Academy of Sciences 104 (2007) 20708–20712.
[39] X. Shen, J.M. Collier, M. Hlaing, L. Zhang, E.H. Delshad, J. Bristow, H.S. Bernstein, Genome-wide examination of myoblast cell cycle withdrawal during differentiation, Developmental Dynamics 226 (2003) 128–138.
[40] V. Andrés, K. Walsh, Myogenin expression, cell cycle withdrawal, and phenotypic differentiation are temporally separable events that precede cell fusion upon myogenesis, The Journal of Cell Biology 132 (1996) 657–666.